Constraints on collective density variables: One dimension

Yizhong Fan and Jerome K. Percus
Courant Institute of Mathematical Sciences, New York University, 251 Mercer Street, New York, New York 10012

Dorothea K. Stillinger and Frank H. Stillinger
AT&T Bell Laboratories, Murray Hill, New Jersey 07974

(Received 21 February 1991)

Collective density variables $\rho(\mathbf{k})$ are frequently employed in many-body physics to describe a wide variety of static and dynamic phenomena. These variables are nonlinear functions of particle positions, and consequently exhibit subtle couplings and kinematic constraints. We examine some of these features for one-dimensional systems, using both numerical exploration and analytical techniques. In particular we have considered the consequences of quenching density fluctuations [minimizing the $\rho(k)$'s] for sets of wave vectors surrounding the origin. This is shown, under proper circumstances, to force other sets of $\rho(k)$'s automatically to their minima, and even to induce perfect crystallization of the many-particle system.

I. INTRODUCTION

The distribution of matter encountered in many-particle systems often finds its most natural expression in terms of collective density variables. For N identical point particles at positions $\mathbf{r}_1, \ldots, \mathbf{r}_N$ within a D-dimensional box Ω, these collective variables are conventionally defined by

$$\rho(\mathbf{k}) = \sum_{j=1}^{N} \exp(i\mathbf{k}\cdot\mathbf{r}_j) \ . \tag{1.1}$$

The $\mathbf{k}$ are wave vectors appropriate for Ω. Examples abound in the physics literature of the utility of the $\rho(\mathbf{k})$ as collective variables; illustrative cases are provided by the random-phase approximation for conduction electrons in metals [1], the study of phonons in superfluid helium [2], detection of nucleation and crystal growth in simulations for supercooled melts [3], and derivation of self-consistent integral equations for pair correlation functions in classical fluids [4,5]. But in spite of their broad applicability and frequent use, collective density variables remain a mathematically underexplored subject. The present paper is intended as a modest start toward rectifying that weakness.

Section II provides some definitions and elementary relations, presented in a form valid for arbitrary integer dimension $D \geq 1$. Although we intend to address in detail the $D > 1$ cases in due course, this paper concentrates on the relatively simple behavior for $D = 1$. Section III presents results of high-precision numerical experiments in one dimension that reveal some nontrivial aspects of the coupling between $\rho(k)$'s. This is followed in Sec. IV and V by the derivation and exploitation of a family of sum rules for the collective density variables. These sum rules generate a rationale for some of the numerical patterns identified in Sec. III. Finally, Sec. VI offers discussion and a few concluding remarks.

II. ELEMENTARY RELATIONS

Only the $\mathbf{k}=0$ collective variable is independent of particle positions $\mathbf{r}_1, \ldots, \mathbf{r}_N$:

$$\rho(0) \equiv N \ . \tag{2.1}$$

All others are complex, with

$$\rho(-\mathbf{k}) = \rho^*(\mathbf{k}) \ , \tag{2.2}$$

and have amplitudes that fluctuate between (attainable) upper and lower limits as the N particles move about:

$$0 \leq |\rho(\mathbf{k})| \leq N \quad (\mathbf{k} \neq 0) \ . \tag{2.3}$$

It is conventional to suppose that the box Ω is a D-dimensional rectangular solid to which periodic boundary conditions apply, i.e., Ω and its periodic images fill the space. If any particle configuration is uniformly translated, only the phase angles of the $\mathbf{k} \neq 0$ collective variables change, not their magnitudes. Consequently, it is useful to introduce the real function $C(\mathbf{k})$ which measures those magnitudes:

$$\begin{aligned} &\rho(\mathbf{k})\rho(-\mathbf{k}) = |\rho(\mathbf{k})|^2 = N + 2C(\mathbf{k}) \ , \\ &C(\mathbf{k}) = \sum_{j<l=1}^{N} \cos[\mathbf{k}\cdot(\mathbf{r}_j - \mathbf{r}_l)] \ . \end{aligned} \tag{2.4}$$

Clearly we have

$$\begin{aligned} &C(0) = \tfrac{1}{2}N(N-1) \ , \\ &C(-\mathbf{k}) = C(\mathbf{k}) \ , \\ &-\tfrac{1}{2}N \leq C(\mathbf{k}) \leq \tfrac{1}{2}N(N-1) \quad (\mathbf{k} \neq 0) \ . \end{aligned} \tag{2.5}$$

Let $v(\mathbf{r})$ be a translation- and inversion-invariant particle pair potential with Fourier transform $V(\mathbf{k})$:

$$V(\mathbf{k})=\int_{\Omega}d\mathbf{r}\,v(\mathbf{r})\exp(i\mathbf{k}\cdot\mathbf{r}) ,$$
$$v(\mathbf{r})=\Omega^{-1}\sum_{\mathbf{k}}V(\mathbf{k})\exp(-i\mathbf{k}\cdot\mathbf{r}) . \tag{2.6}$$

The total interaction for all pairs of particles in the N-body system may be written in the following equivalent forms:

$$\Phi=\sum_{j<l=1}^{N}v(\mathbf{r}_j-\mathbf{r}_l)$$
$$=(2\Omega)^{-1}\sum_{\mathbf{k}}V(\mathbf{k})[\rho(\mathbf{k})\rho(-\mathbf{k})-N]$$
$$=\Omega^{-1}\sum_{\mathbf{k}}V(\mathbf{k})C(\mathbf{k}) . \tag{2.7}$$

A specific choice of interaction that will be useful in the following is the $\mathbf{k}$-space square mound potential:

$$V(\mathbf{k})=\begin{cases}V_0>0 & (|\mathbf{k}|\le K)\\ 0 & (K<|\mathbf{k}|) .\end{cases} \tag{2.8}$$

In this case Φ depends on only the finite set of collective variables with wave-vector magnitudes at or below the cutoff K.

In the large-Ω limit (K fixed), the second of Eqs. (2.6) reduces to a standard integral form for evaluation of $v(\mathbf{r})$:

$$\lim_{\Omega\to\infty}v(\mathbf{r})=V_0(K/2\pi r)^{D/2}J_{D/2}(Kr) , \tag{2.9}$$

where J_ν is the Bessel function of the first kind [6]. This potential is bounded, oscillatory, and displays an algebraic decay with increasing distance r. Specific forms for $D=1,2$, and 3 are the following:

$$v_1(r)=(V_0/\pi r)\sin(Kr) ,$$
$$v_2(r)=(V_0K/2\pi r)J_1(Kr) , \tag{2.10}$$
$$v_3(r)=(V_0/2\pi^2r^3)[\sin(Kr)-Kr\cos(Kr)].$$

Since v is inversion symmetric, so too is V. Consequently the number of $\mathbf{k}$'s for which $V(\mathbf{k})$ in Eq. (2.8) is positive must be an odd integer, say $2M+1$:

$$V_0^{-1}\sum_{\mathbf{k}}V(\mathbf{k})=2M+1 , \tag{2.11}$$

If M is sufficiently small compared to N, it is reasonable to expect (and indeed is confirmed in later sections) that particle configurations in Ω would exist for which simultaneously

$$|\rho(\mathbf{k})|=0 \quad \text{for all } 0<|\mathbf{k}|\le K . \tag{2.12}$$

In other words, the N particles could be placed so as to suppress completely the density variations with wavelengths contributing nontrivially to Φ, Eq. (2.7). Let $S(M)$ stand for the set of configurations $\mathbf{r}_1,\ldots,\mathbf{r}_N$ with this property. By definition this is the set of configurations for which Φ attains its absolute minimum:

$$\min_{(\mathbf{r}_1,\ldots,\mathbf{r}_N)}\Phi=(V_0N/2\Omega)(N-2M-1) , \tag{2.13}$$

the system's classical ground state.

It is clear that $S(0)$ includes all particle configurations, and that

$$S(M_1)\subseteq S(M_2) \quad (M_1>M_2) . \tag{2.14}$$

If $S(M)$ contains configuration $\mathbf{r}_1,\ldots,\mathbf{r}_N$, it also contains all configurations that can be generated from it by uniform translations, by particle permutations, and by the point-group symmetry operations for Ω.

Some basic questions concerning the configuration sets $S(M)$ are the following.

(a) What is the smallest M value (for given N) such that $S(M)$ is empty?

(b) Which nonempty sets are connected?

(c) How does dim $[S(M)]$ vary with M?

(d) How are the $\rho(\mathbf{k})$, or equivalently the $C(\mathbf{k})$, for $|\mathbf{k}|>K$ distributed as a function of M? The numerical investigation reported in Sec. III provides some answers to these queries for $D=1$.

III. NUMERICAL STUDY FOR $D=1$

A relatively complete characterization of the classical ground state for potentials of type (2.8) is possible for the one-dimensional case, provided K is not too large (in a sense to be made clear). In this circumstance $x_1,\ldots,x_N$ can denote particle locations on the line, and we can take Ω to be the line interval

$$0\le x_j<L \quad (j=1,\ldots,N) . \tag{3.1}$$

The wave vectors form a one-dimensional periodic sequence

$$k=0,\pm2\pi/L,\pm4\pi/L,\ldots . \tag{3.2}$$

The one-dimensional perfect "crystal" has a special significance. This corresponds to the arrangement

$$x_j^{(0)}=(j-1)L/N+u , \tag{3.3}$$

or any particle permutation thereof, wherein u is a common displacement satisfying

$$0\le u<L/N , \tag{3.4}$$

but is otherwise arbitrary. One immediately finds for this regular arrangement that

$$\rho(k)=N\exp(iku)\sum_{n=-\infty}^{\infty}\delta_K(k-2\pi nN/L) , \tag{3.5}$$

where δ_K is the Kronecker delta. Hence the $\rho(k)$ all vanish except those at the "Bragg" points [7]

$$k(\text{Bragg})=2\pi nN/L \quad (n=0,\pm1,\pm2,\ldots) , \tag{3.6}$$

for which the $\rho(k)$ achieve their maximum possible magnitude N [cf. Eq. (2.3)]. The corresponding pattern for the real quantities $C(k)$ is that they are at their minimum $(-\frac{1}{2}N)$ or maximum $[\frac{1}{2}N(N-1)]$, respectively, for k values away from, or at, the Bragg points. The obvious implication of these remarks is that all perfect crystal arrangements in one dimension belong to the configuration sets $S(M)$ for $M<N$.

Recall that periodic boundary conditions apply. Thus

free translation can convert any particle ordering in a crystalline array into $N-1$ others. This implies that the full set of crystalline particle arrangements in one dimension constitute $(N-1)!$ disconnected manifolds each of dimension 1 in the full N-dimensional configuration space.

The potential energy for the one-dimensional system with square mound $V(k)$ may be written as follows:

$$\Phi/V_0 = N(N-1)/2L + (2/L)\sum_{m=1}^{M} C(2\pi m/L) . \tag{3.7}$$

Our numerical study has been directed toward generating representative configurations in the sets $S(M)$. Starting with randomly assigned particle positions, steepest-descent trajectories on the multidimensional Φ hypersurface were produced, the end product of which (if successful) would be a system configuration for which each C in the sum in Eq. (3.7) would attain its minimum $-N/2$. The resulting collection of particle configurations for various N and M were then analyzed to illuminate questions (A)–(D) at the end of Sec. II.

As a final preliminary to discussion of the numerical results, we consider the effect on the collective variables of small distortions from the perfect crystalline arrangement. Therefore generalize Eq. (3.3) to

$$x_j = (j-1)L/N + u + s_j , \tag{3.8}$$

where the s_j will be treated as infinitesimals. The requirement that all of the C's in expression (3.7) be simultaneously at their minima gives rise to the following simultaneous equations after linearizing with respect to the s_j:

$$\begin{aligned} &\sum_{j=1}^{N} \sin(2\pi mj/N)s_j = 0 , \\ &\sum_{j=1}^{N} \cos(2\pi mj/N)s_j = 0, \quad m = 1,2,\ldots,M . \end{aligned} \tag{3.9}$$

If $M < N/2$, these equations are linearly independent and provide $2M$ constraints on the N variables $s_1,\ldots,s_N$; consequently the dimension of the configuration set $S(M)$ in the immediate neighborhood of any crystal configuration must be $N-2M$. However, if N is even and $m = M = N/2$, all coefficient sines in the first of Eqs. (3.9) vanish to yield one fewer constraint; in this case the local dimension of $S(N/2)$ near crystallinity is one, presumably corresponding just to uniform translation. Increasing M into the range $N/2 < M < N$ does not produce more constraints, but merely replicates those already in hand. The local dimension of $S(M)$ thus is given by the expression

$$\max(N-2M,1) \quad (0 \le M < N) . \tag{3.10}$$

One of the tasks of numerical investigation is to validate this expression as the global dimension of $S(M)$ throughout the N-dimensional configuration space.

Evidently $S(N)$ is empty. The most uniform distribution of N particles on a line is the periodic crystalline array, and this inevitably generates Bragg maxima at the points (3.6). No particle configuration exists permitting a wider range of k values surrounding the origin to have totally suppressed density fluctuations.

Our steepest-descent numerical studies have included many system sizes in the range $2 \le N \le 100$, various M values primarily in the range $1 \le M \le N/2$, and collections of random initial configurations for each N,M as seemed appropriate and feasible. Calculations were carried out to high precision, with the configuration-dependent part of Φ typically converged to its absolute minimum to 12 significant figures. The following general comment should be noted: For all N examined, and with $M < N$, the steepest-descent trajectories always converged to the absolute Φ minimum. Evidently the Φ hypersurface contains no relative minima lying above the classical ground state.

The pattern of results obtained is clear and systematic. We believe it extends to all $N \ge 2$.

The calculations show that when M is in the range

$$\begin{aligned} &N/2 \le M \le N-1 \quad (N \text{ even}) , \\ &(N-1)/2 \le M \le N-1 \quad (N \text{ odd}) , \end{aligned} \tag{3.11}$$

only a perfect crystalline arrangement permits Φ to attain its absolute minimum. This confirms the prior suggestion based on linear constraints (3.9). However irregular the initial particle configuration might be, the steepest-descent minimization in this family of cases (3.11) invariably spaces the particles evenly on the line. Thus it is only necessary to suppress density fluctuations about halfway from the origin in k space to the nearest k(Bragg) to force the one-dimensional system to crystallize.

Next we consider the M ranges

$$\begin{aligned} &0 \le M \le [(N-2)/3] \quad (N \text{ even}) . \\ &0 \le M \le [(2N-3)/6] \quad (N \text{ odd}) , \end{aligned} \tag{3.12}$$

where [ ] denotes "integer part." Here only those $C(k)$'s within the range of the square mound $V(k)$ are forced to equal the minimum $-N/2$. All others seem to be free to vary between the limits shown in Eq. (2.5). Examination of particle configurations emerging from the steepest-descent procedure shows them to be quite disordered, typically without any hint of crystallinity. Obviously a wide range of configurations belong to the corresponding $S(M)$ of which the displacements s_j, Eq. (3.8), are large and only weakly correlated at most.

The least obvious and therefore most intriguing behavior develops in the intermediate regime:

$$\begin{aligned} &[(N-2)/3] < M < N/2 \quad (N \text{ even}) , \\ &[(2N-3)/6] < M < (N-1)/2 \quad (N \text{ odd}) . \end{aligned} \tag{3.13}$$

As M increases from the lower to the upper end of the range indicated, more and more intervals of contiguous k values arise, appearing farther and farther from the origin, in which the $C(k)$ have been implicitly forced to their lower limit $-N/2$. This occurs even though the k values involved lie outside the range of $V(k)$. Thus the intermediate regime (3.13) systematically interpolates the small-M case where only $C(k)$'s within the range of $V(k)$ are minimized, to the large-M case where all $C(k)$'s are minimized except for those at the Bragg points.

Confine attention for the moment to N an even integer. Set

$$M=N/2-l \quad (N \text{ even}) \tag{3.14}$$

so that when

$$1\leq l\leq N/2-[(N+1)/3] \tag{3.15}$$

the variations in l span the intermediate regime. We have found that starting from the first positive k value and proceeding along the positive k axis, the alternating intervals respectively of minimal and of nonminimal $C(k)$'s have lengths that follow simple arithmetic progressions. Specifically the sequence runs as follows:

$$\begin{aligned}
&N/2-l \text{ minimal } C(k)\text{'s} ,\\
&(2l-2)+1 \text{ nonminimal } C(k)\text{'s} ,\\
&(N/2-l)-(2l-2) \text{ minimal } C(k)\text{'s} ,\\
&2(2l-2)+1 \text{ nonminimal } C(k)\text{'s} ,\\
&(N/2-l)-2(2l-2) \text{ minimal } C(k)\text{'s} ,\\
&3(2l-2)+1 \text{ nonminimal } C(k)\text{'s} ,
\end{aligned} \tag{3.16}$$

etc. The progressions continue unless or until the length of the interval of minimal $C(k)$'s vanishes, and beyond that point an uninterrupted infinite sequence of nonminimal $C(k)$'s appear.

The behavior just described is particularly simple when $l=1$. Then the only nonminimal $C(k)$'s are those at the Bragg points (3.6) *and* at the k's midway between successive Bragg points. The system configurations are those of two independently translatable sublattices each containing half of the particles, e.g.,

$$\begin{aligned}
&x_{2j-1}=(2j-2)L/N+u_1 ,\\
&x_{2j}=(2j-1)L/N+u_2, \quad (1\leq j\leq N/2) .
\end{aligned} \tag{3.17}$$

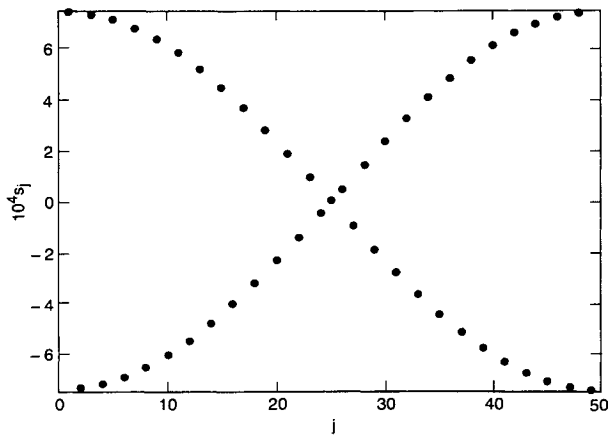

FIG. 1. Particle displacements s_j vs j for the case $N=49$, $l=1$ (i.e., $M=23$). The particles are arranged in order along the system with length $L=1$. The displacements shown are measured relative to a perfect crystalline arrangement. The configuration amounts to a small-amplitude, modulated Brillouin-zone-boundary phonon.

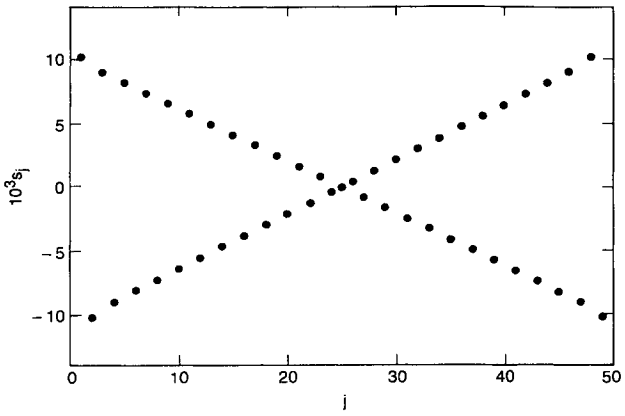

FIG. 2. Particle displacements s_j vs j for the case $N=49$, $l=1$ (i.e., $M=23$), corresponding to a large-amplitude modulated Brillouin-zone-boundary phonon. This should be compared to the contrasting small-amplitude case displayed in Fig. 1.

The presence of the two independent sublattice displacements u_1 and u_2 makes it clear that the global dimension of the corresponding configuration set $S(N/2-1)$ is 2, in agreement with the local dimension implied earlier by the constraint equations, (3.9). Note that the two sublattices can be translated into coincidence and then particles permuted between them; in this way all configurations can be continuously deformed to one another so the set $S(N/2-1)$ is fully connected.

The odd-N cases are quite similar, but require slight notational changes. Now set

$$M=(N-1)/2-l \quad (N \text{ odd}) \tag{3.18}$$

so that the intermediate regime specified by the second of relations (3.13) is spanned by

$$1\leq l\leq [N/6] . \tag{3.19}$$

Once again, starting from the first positive k value and proceeding along the positive-k axis, alternating intervals of minimal and of nonminimal $C(k)$'s have lengths in arithmetic progression (at least until the former vanish). Now one finds, for odd N, that the sequence is

$$\begin{aligned}
&(N-1)/2-l \text{ minimal } C(k)\text{'s} ,\\
&(2l-2)+2 \text{ nonminimal } C(k)\text{'s} ,\\
&(N-1)/2-l-(2l-1) \text{ minimal } C(k)\text{'s} ,\\
&2(2l-2)+3 \text{ nonminimal } C(k)\text{'s} ,\\
&(N-1)/2-l-2(2l-1) \text{ minimal } C(k)\text{'s} ,\\
&3(2l-2)+4 \text{ nonminimal } C(k)\text{'s} ,
\end{aligned} \tag{3.20}$$

etc. The preceding argument for infinitesimal displacements suggests that for N odd, $l=1$ [i.e., $M=(N-3)/2$], the dimension of the configuration set should be 3. The numerical work confirms that this is indeed the case even for finite displacements. Figures 1 and 2 help to illustrate this point by showing two collections of displacements obtained numerically for $N=49$, $l=1$. As in Eq.

(3.8) above, these displacements are reckoned as relative to a perfect reference lattice, and have the character of a zone-boundary phonon with a long-wavelength modulation that just accommodates the odd number of particles. The three degrees of freedom present are (a) the uniform translation mode, (b) the amplitude of the modulated phonon, and (c) the phase of the modulation. For the small-amplitude example displayed in Fig. 1 the modulation envelope is nearly a pure sinusoid. By contrast the large-amplitude example in Fig. 2 possesses essentially a peaked triangular-wave envelope. Intermediate amplitude cases interpolate between these extremes.

IV. EXACT SUM RULES: PRELIMINARY

The intriguing results of Sec. III suggest that, lurking beneath the surface, are analytical relationships among the collective variables. To avoid unnecessary notational complexity we will now adopt units such that $L=2\pi$; then the index in ρ_m is an integer and the $\{x_j\}$ can be regarded as angles.

An indication that non-numerical analysis might be fruitful emerges immediately from the elementary example $N=4$, $l=1$, (i.e., $M=1$). Here we have

$$\rho_1=\sum_{j=1}^{4}\exp(ix_j)=0\ . \tag{4.1}$$

The separate terms in this sum are unit vectors in the complex plane, and in order for them to add to zero, they must geometrically form a rhombus. When raised to any positive or negative odd power, say $2n-1$, the pairs of antiparallel vectors forming opposite sides of this rhombus rotate in the complex plane, but remain antiparallel. Consequently another rhombus is formed, and so

$$\rho_{2n-1}=0\ . \tag{4.2}$$

For an even index, the corresponding powers produce parallel opposite sides which do not cancel. Hence minimal and nonminimal C_m's alternate with m, in exact accord with the scheme (3.16) above.

The elementary example just discussed clearly involves constraints on higher-order moments of a set of discrete variables—the $y_j\equiv\exp(ix_j)$—given low-order moments. A general procedure for addressing this kind of problem was first devised by I. Newton [8], whose approach we now review briefly and then extend to the collective variable relationships at issue. Given N independent variables $y_1,\cdots,y_N$, define

$$S_n=\sum_{i=1}^{N}y_i^n\ . \tag{4.3}$$

At most N of these sums can be independently specified; all others can in principle be expressed as functions of the N fixed S_n's.

We start by representing the $\{y_j\}$, whose order is immaterial, by the generating function

$$\begin{aligned}f(z)&=\prod_{i=1}^{N}(1-zy_i)\\&=\sum_{j=0}^{N}a_jz^j\ ,\end{aligned} \tag{4.4}$$

where $a_0\equiv 1$. It follows that

$$\begin{aligned}\ln f(z)&=\sum_{i=1}^{N}\ln(1-zy_i)\\&=-\sum_{i=1}^{N}\sum_{n=1}^{\infty}y_i^nz^n/n\\&=-\sum_{n=1}^{\infty}S_nz^n/n\ .\end{aligned} \tag{4.5}$$

There are several ways in which Eq. (4.5) can be employed. To establish Newton's relations, we observe that

$$\begin{aligned}\frac{d}{dz}\ln f(z)&=f'(z)/f(z)\\&=-\sum_{n=1}^{\infty}S_nz^{n-1}\ ,\end{aligned} \tag{4.6}$$

or equivalently

$$f'(z)+f(z)\sum_{n=1}^{\infty}S_nz^{n-1}=0\ . \tag{4.7}$$

Utilizing Eq. (4.4), this last relation can be written out explicitly as

$$\sum_{j=1}^{N}ja_jz^{j-1}+\sum_{n=1}^{\infty}\sum_{j=n}^{N+n}a_{j-n}S_nz^{j-1}=0\ . \tag{4.8}$$

Adopting the notation, consistent with (4.4), that

$$a_j=0\quad\text{for } j<0 \text{ or } j>N\ , \tag{4.9}$$

Eq. (4.8) simplifies to

$$\sum_{j=1}^{\infty}z^{j-1}(ja_j+\sum_{n=1}^{\infty}a_{j-n}S_n)=0\ , \tag{4.10}$$

which, since z is arbitrary, yields Newton's result

$$ja_j+\sum_{n=1}^{\infty}a_{j-n}S_n=0\quad(j=1,2,3,\ldots)\ . \tag{4.11}$$

Equation (4.11), taken at $j=1,\ldots,N$, iteratively expresses $a_1,\ldots,a_N$ in terms of $S_1,\ldots,S_N$. A typical question it might be used to answer would be the following: How can S_{N+1} be expressed in terms of $S_1,\ldots,S_N$? The response could either involve solving the $(N+1)$st equation for S_{N+1}:

$$S_{N+1}=-\sum_{n=1}^{N}a_{N+1-n}(S_1,\ldots,S_N)S_N\ , \tag{4.12}$$

or, without bothering to solve for the $\{a_j\}$, could instead observe that the first $N+1$ equations formally constitute a homogeneous linear system on $N+1$ variables: $1,a_1,\ldots,a_N$, whose determinant must thereby vanish. However, there is a more direct approach, based on Eq. (4.5), in the form

$$f(z)=\exp\left[-\sum_{n=1}^{\infty} S_n z^n/n\right] . \tag{4.13}$$

Since $f(z)$ is of degree N in z, we can rewrite (4.13) as

$$f(z)=P_N \exp\left[-\sum_{n=1}^{\infty} S_n z^n/n\right] , \tag{4.14}$$

where P_N is the projection onto Nth order polynomials:

$$P_N \sum_{j=0}^{\infty} g_j z^j = \sum_{j=0}^{N} g_j z^j . \tag{4.15}$$

Thus $f(z)$ is expressed in terms of the $S_1,\ldots,S_N$ alone, and we can reapply (4.5) to get

$$\sum_{n=1}^{\infty} S_n z^n/n = -\ln\left[P_N \exp\left[-\sum_{n=1}^{N} S_n z^n/n\right]\right] , \tag{4.16}$$

whose expansion recovers any S_n in terms of $S_1,\ldots,S_N$.

V. EXACT SUM RULES

The collective variables of interest, the ρ_k, are indeed moments of the $y_j=\exp(ix_j)$, but both positive and negative powers are included. Suppose that $N=2\bar{N}$ is even; then the information given is that of $\rho_{\pm 1},\ldots,\rho_{\pm\bar{N}}$. The subset of Eqs. (4.11)

$$ja_j+\sum_{n=1}^{j} a_{j-n}\rho_n=0 , \quad (j=1,\ldots,\bar{N}) \tag{5.1}$$

now determines $a_1,\ldots,a_{\bar{N}}$ in terms of $\rho_1,\ldots,\rho_{\bar{N}}$, but $a_{\bar{N}+1},\ldots,a_{2\bar{N}}$ remain to be found. For this purpose we also examine the generating function

$$g(z)=\prod_{i=1}^{N}(1-z/y_i) = \sum_{j=0}^{N} b_j z^j . \tag{5.2}$$

By following the same procedure as before, we are led to

$$jb_j+\sum_{n=1}^{\infty} b_{j-n}\rho_{-n}=0 , \tag{5.3}$$

so that, using the easily established identities

$$a_N b_j = a_{N-j} , \tag{5.4}$$

we have

$$ja_{N-j}+\sum_{n=1}^{j} a_{N-j+n}\rho_{-n}=0 \quad (j=1,\ldots,N-1) . \tag{5.5}$$

This evaluates $a_{\bar{N}+1},\ldots,a_{2\bar{N}-1}$ in terms of $\rho_{-1},\ldots,\rho_{-\bar{N}}$, to which

$$a_{2\bar{N}}=\exp\left[i\sum_{j=1}^{N} x_j\right] \tag{5.6}$$

is appended, serving as an undetermined phase factor.

There is now no problem in principle to computing the ρ_j for $j>\bar{N}$ in terms of $\rho_{\pm 1},\ldots,\rho_{\pm\bar{N}}$. We use (4.11) in the form

$$\rho_j=-\sum_{n=1}^{j-1} a_{j-n}\rho_n - ja_j \tag{5.7}$$

and iterate, starting at $j=\bar{N}+1$. If many of the set $(\rho_{\pm 1},\ldots,\rho_{\pm\bar{N}})$ vanish, the task is substantially simplified. For example, consider the case $M=\bar{N}$ of Sec. III, i.e.,

$$\rho_{\pm 1}=\rho_{\pm 2}=\cdots=\rho_{\pm\bar{N}}=0 . \tag{5.8}$$

Equations (5.1) and (5.5) then imply at once that

$$a_1=a_2=\cdots=a_{N-1}=0 . \tag{5.9}$$

Subsequently setting $j=\bar{N}+1,\ldots,N-1$ in (5.7) leads to

$$\rho_{\bar{N}+1}=\cdots=\rho_{N-1}=0 , \tag{5.10}$$

while $j=N$ in (5.7) then yields $\rho_N=-Na_N$, or since a_N is just a unit vector,

$$|\rho_N|=N . \tag{5.11}$$

Continuing the process, one easily verifies for this case that

$$|\rho_n|=N\sum_{j=-\infty}^{\infty}\delta_K(n-jN) , \tag{5.12}$$

where as before δ_K is the Kronecker delta. Thus we have verified that the only nonminimal ρ_n's are those at the Bragg points, i.e., enforcing $M=\bar{N}=N/2$ indeed creates only a perfect crystal as indicated by the numerical study.

Cases with smaller M proceed similarly, although with increased complexity. For a systematic description, it is best to generalize the direct expansion of (4.16) to the collective coordinates. Let us now suppose that N is odd, $N=2\bar{N}+1$, and for minor notational convenience introduce the "normalized" collective variables

$$q_k=\rho_k/k \quad (k\neq 0) . \tag{5.13}$$

We will regard $q_{\pm 1},\ldots,q_{\pm\bar{N}}$ together with the phase factor

$$\omega=\exp\left[i\sum_{j=1}^{N} x_j\right] \tag{5.14}$$

as our basic independent variables. We start by copying (4.13) as

$$\prod_{j=1}^{N}(1-y_j z)=\sum_{j=0}^{2\bar{N}+1} a_j z^j = \exp\left[-\sum_{n=1}^{\infty} q_n z^n\right] , \tag{5.15}$$

but instead of proceeding to form (4.14), we project out only through $z^{\bar{N}}$:

$$\sum_{j=0}^{\bar{N}} a_j z^j = P_{\bar{N}} \exp\left[-\sum_{n=1}^{\bar{N}} q_n z^n\right] . \tag{5.16}$$

Letting $y_j\to 1/y_j$, $z\to 1/z$ in (5.15), we also have

$$\prod_{j=1}^{N}[1-1/(y_j z)]=-(1/\omega)z^{-N}\prod_{j=1}^{N}(1-y_j z)$$
$$=\exp\left[\sum_{n=1}^{\infty}q_{-n}z^{-n}\right], \tag{5.17}$$

so that

$$\prod_{j=1}^{N}(1-y_j z)=\sum_{j=0}^{N}a_j z^j$$
$$=-\omega z^N\exp\left[\sum_{n=1}^{\infty}q_{-n}z^{-n}\right]. \tag{5.18}$$

It follows that, in obvious notation,

$$\sum_{j=\bar{N}+1}^{N}a_j z^j=-\omega z^N P_{-\bar{N}}\exp\left[\sum_{n=1}^{\bar{N}}q_{-n}z^{-n}\right]. \tag{5.19}$$

Hence combining Eqs. (5.15), (5.16), and (5.19) we arrive at the identity

$$\sum_{n=1}^{\infty}q_n z^n=-\ln\left[P_{\bar{N}}\exp\left[-\sum_{n=1}^{\bar{N}}q_n z^n\right]\right.$$
$$\left.-\omega z^N P_{-\bar{N}}\exp\left[\sum_{n=1}^{\bar{N}}q_{-n}z^{-n}\right]\right]. \tag{5.20}$$

A number of consequences flow easily from (5.20) to shed further light upon our numerical investigations. To begin, suppose that

$$\rho_n=0 \quad \text{for } |n|\le\bar{N}-l,\ l<\bar{N}/2\ . \tag{5.21}$$

Then the argument [ ] of the logarithm in (5.20) takes the form

$$\sum_{n=\bar{N}-l+1}^{\bar{N}+l}c_n z^n+\omega z^N\ ,$$

and (5.20) thus implies that for $l>0$,

$$\rho_n\neq 0 \quad \text{only if } (\bar{N}-l+1)p\le|n|\le(\bar{N}+l)p\ ,$$
$$p=1,2,3,\ldots\ . \tag{5.22}$$

In other words, there are nonzero sequences of length $(2l-1)p+1$ interspersed with zero sequences of length $\bar{N}-l-(2l-1)p$. The first nonimposed zero sequence $p=1$ is absent unless $\bar{N}-l-(2l-1)>0$, i.e., $l<(\bar{N}+1)/3=(N+1)/6$.

For small l in (5.21), one can make a much more detailed characterization. First, let $l=0$, the special case excluded from (5.22). Then (5.20) reads

$$\sum_{n=1}^{\infty}q_n z^n=-\ln(1-\omega z^N)\ , \tag{5.23}$$

so that only the

$$\rho_{Np}=\omega^p N \tag{5.24}$$

are nonvanishing—a perfect crystal with center of mass $\sum_j x_j/N$.

Next, let $l=1$, in which case

$$\sum_{n=1}^{\infty}q_n z^n=-\ln(1-q_{\bar{N}}z^{\bar{N}}-\omega q_{-\bar{N}}z^{\bar{N}+1}-\omega z^{2\bar{N}+1})\ , \tag{5.25}$$

and the associated configuration space $S[(N-3)/2]$ is determined by three parameters ω, $q_{\bar{N}}$, and $q_{-\bar{N}}$. On the one hand, we can find explicitly the full set of $\{q_n\}$. To do so it is convenient to remove the effect of the center-of-mass position by setting

$$\hat{q}_n=q_n/\omega^{n/N} \tag{5.26}$$

while concurrently letting $z\to z\omega^{1/N}$. This eliminates ω in (5.25):

$$\sum_{n=1}^{\infty}\hat{q}_n z^n=-\ln(1-\hat{q}_{\bar{N}}z^{\bar{N}}-\hat{q}_{-\bar{N}}z^{\bar{N}+1}-z^{2\bar{N}+1})\ , \tag{5.27}$$

and in fact does the same in the general expression (5.20). Thus expanding (5.20) in multinomial form,

$$\sum_{n=1}^{\infty}\hat{q}_n z^n=\sum_{s,t,u}\frac{(s+t-u-1)!}{(s-u)!(t-u)!u!}$$
$$\times\hat{q}_{\bar{N}}^{s-u}\hat{q}_{-\bar{N}}^{t-u}z^{s\bar{N}+t(\bar{N}+1)}\ . \tag{5.28}$$

If $n<\bar{N}^2$, the nonvanishing $\hat{q}_n$ appear as $(p+1)$ triplets, with $s=p-t$, $0\le t\le p$, $n=p\bar{N}+t$, or

$$\hat{q}_{p\bar{N}+t}=\sum_{u}\frac{(p-u-1)!}{(p-t-u)!(t-u)!u!}\hat{q}_{\bar{N}}^{p-t-u}\hat{q}_{-\bar{N}}^{t-u}\ . \tag{5.29}$$

We are also in a position to analyze the x-space configurations associated with $l=1$, as illustrated in Figs. 1 and 2. Since

$$\prod_{j=1}^{N}\left[1-z\exp(ix_j)\right]=1-\hat{q}_{\bar{N}}z^{\bar{N}}-\hat{q}_{-\bar{N}}z^{\bar{N}+1}-z^{2\bar{N}+1}\ , \tag{5.30}$$

we need the possible sets of roots of the foregoing polynominal. Setting

$$\hat{q}_{\bar{N}}=\rho_{\bar{N}}/\bar{N}=r\exp(-i\phi/2)\ ,$$
$$z=\exp(-ix)\ , \tag{5.31}$$

these are given by

$$\sin(Nx/2)=r\sin[(x-\phi)/2]\ , \tag{5.32}$$

which is plotted in Fig. 3 for various values of r. At $r=0$, i.e., $\rho_{\pm 1}=\cdots=\rho_{\pm N}=0$, we of course have the perfect crystal:

$$x_j^{(0)}=2\pi j/N \quad (j=0,\ldots,N-1)\ . \tag{5.33}$$

For small r, Eq. (5.32) is solved to leading order by

$$x_j=x_j^{(0)}+(-1)^j(2r/N)\sin[(x_j^{(0)}-\phi)/2]\ , \tag{5.34}$$

a pair of half-wave sinusoidal distributions. As r increases, the trigonometric form distorts increasingly until

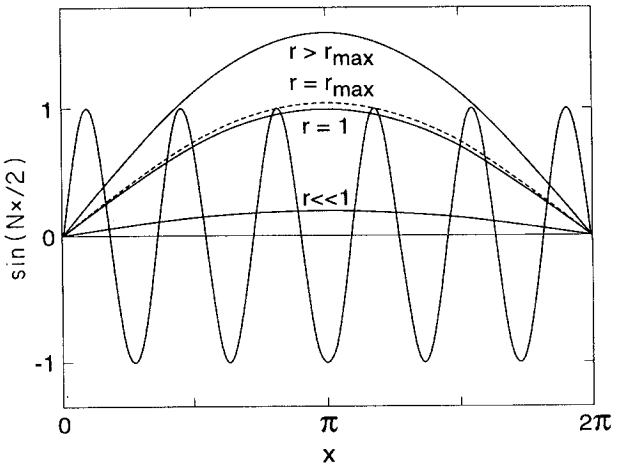

FIG. 3. Graphical solution of Eq. (5.32) for various values of the parameter r. Here $N=11$, $\phi=0$.

at $r=1$ we have

$$\sin(Nx/2)-\sin[(x-\phi)/2] = 2\sin\left[\frac{(N-1)x+\phi}{4}\right]\cos\left[\frac{(N+1)x-\phi}{4}\right] = 0 , \tag{5.35}$$

so that

$$x_j=\frac{2\pi j-(-1)^j\phi}{N-(-1)^j} . \tag{5.36}$$

This last result represents an interwoven pair of perfectly crystalline configurations, one for $\bar{N}$ particles, the other for $\bar{N}+1$. The deviations from $x_j^{(0)}$ are then of course one positive linear function and one negative linear function of j.

If r is too large, then Fig. 3 shows that there will be fewer than N real roots (the others move into the complex plane in pairs), an impermissible situation. The maximum allowable r is clearly achieved when the maximum of $\sin[(x-\phi)/2]$ occurs at the minimum of $\sin(Nx/2)$; for odd N this will be $x=\pi$ when $\phi=0$. Thus $\sin(Nx/2)=r\sin(x/2)$. But the two points of tangency clearly satisfy $|x-\pi|<3\pi/2N$. Hence

$$\begin{aligned} r^2&=\sin^2(Nx/2)/\sin^2(x/2) \\ &<1/\sin^2(x/2) \\ &=1/\{1-\sin^2[(x-\pi)/2]\} , \end{aligned} \tag{5.37}$$

giving

$$r_{\max}^2<1/[1-(3\pi/4N)^2] , \tag{5.38}$$

rapidly approaching 1 for large N. Thus, when $l=1$ holds, we also have the kinematic constraint

$$\rho_{\bar{N}}\rho_{-\bar{N}}<\bar{N}^2/[1-(3\pi/4N)^2] . \tag{5.39}$$

We surmise that at large N, the constraints until moderate values of l are achieved are all associated with interwoven perfectly crystalline particle subgroups, but we have not been able to prove this.

VI. DISCUSSION

Both numerical and analytical aspects of the present study demonstrate the existence of subtle kinematic constraints acting among collective density variables. Specifically we have found that requiring certain sets of $\rho(k)$'s in one dimension to vanish [or equivalently forcing the corresponding $C(k)$'s to their minima] automatically causes the same to happen for other $\rho(k)$'s [equivalently the $C(k)$'s]. By entirely suppressing density fluctuations halfway to the k(Bragg) nearest the origin, one causes formation of a perfect "crystalline" arrangement in one-dimensional systems of particles.

It should not escape notice that such kinematic constraints, or nonlinear couplings, among collective density variables could have profound implications for the proper form of Landau energy (or free energy) functions [9], which are conventionally written as simple multinomial combinations of the $\rho(k)$'s. Considering the fact that the Landau approach has played such a prominent role in fundamental phase transition theory both for ordinary crystallization [10] and in the study of quasicrystals [11], it is obviously important to understand the mathematical properties of collective density variables in great depth.

Unfortunately, we do not yet have an analytic characterization of the general configuration sets $S(M)$. Nor of course do we have the general kinematic constraints, such as (5.39), which describe the large scale restrictions of $\{\rho_k,\omega\}$ space, $|k|\le\bar{N}$, and the implied failure of the $\{\rho_k,\omega\}$ to be independently variable over their full ranges $|\rho_k|\le N$. If $\{\rho_k,\omega\}$ space were convex, an amassing of extreme points such as (5.39) would quickly improve our intuition as to the nature of the bounding surface. But this is not the case.

We have seen that ordered configuration space $x_1\le x_2,\cdots\le x_N$ maps onto $\{\rho_k,\omega\}$ space in a 1:1 fashion; hence the boundary of $\{\rho_k,\omega\}$ space occurs for example when $x_2=x_1$. The nature of this boundary is most readily seen in the prototypical case $N=3$. Let us fix the center of mass by setting $\omega=1$, or $x_1+x_2+x_3=0$ (with all x's modulo 2π). We therefore have at the boundary

$$x_1=x , \quad x_2=x , \quad x_3=-2x , \tag{6.1}$$

and the real collective variables

$$c_k=\sum_{j=1}^{3}\cos(kx_j) , \quad s_k=\sum_{j=1}^{3}\sin(kx_j) , \tag{6.2}$$

which replace (ρ_k,ρ_{-k}) for geometric considerations, become in the present case simply

$$\begin{aligned} c&=2\cos x+\cos(2x) , \\ s&=2\sin x-\sin(2x) . \end{aligned} \tag{6.3}$$

As Fig. 4 demonstrates, the boundary is now a curve with three-fold rotational symmetry, far from convex, and is in

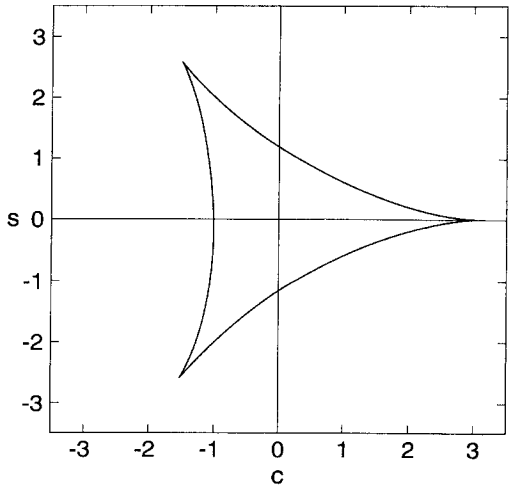

FIG. 4. Accessible (c,s,ω) space for $N=3$ particles at $\omega=0$.

fact bounded by cusps. Extension to $\sum_j x_j \neq 0$ creates a spiral configuration with axis along the $\sum_j x_j$ direction. Here we see that $c^2+s^2=5+4\cos(3x)\geq 1$ on the boundary, so that c and s are in fact independent inside the (c,s) unit circle.

The cusp nature of the $\{\rho_k,\omega\}$ boundary holds for $N>3$ as well. Again suppose $N=2\bar{N}+1$, and consider $C_{\bar{N}}$ near its maximum of N. Then (mod 2π) all x_j are small, and so

$$\begin{aligned} C_{\bar{N}} &= N(1-\epsilon) \\ &= \sum_j \cos(\bar{N}x_j) \\ &= N-\tfrac{1}{2}\bar{N}^2\sum_j x_j^2+\cdots \end{aligned} \tag{6.4}$$

tells us that

$$\begin{aligned} \sum_j x_j^2 &= (2N/\bar{N}^2)\epsilon+\cdots \\ &\sim (8/N)\epsilon \end{aligned} \tag{6.5}$$

to leading order. There are two consequences. The first is that

$$\begin{aligned} C_n &= N-(n^2/2)\sum_j x_j^2+\cdots \\ &\sim N-(4n^2/N)\epsilon\ , \end{aligned} \tag{6.6}$$

restricting space to the immediate vicinity of a hyperplane. The second, assuming again that $\sum_j x_j=0$, is that

$$\begin{aligned} |s_n| &= \left| n\sum_j x_j-\tfrac{1}{6}n^3\sum_j x_j^3+\cdots \right| \\ &< \tfrac{1}{6}n^3N^{1/2}\left[\sum_j x_j^2\right]^{3/2} \end{aligned} \tag{6.7}$$

or

$$s_n<(2^{7/2}/3)(n^3/N)\epsilon^{3/2}\ , \tag{6.8}$$

a cusp within the hyperplane. Thus the surface is very spiky. The generalization to $N>3$ of the existence of the inscribed circle $c^2+s^2<1$ of independent variation for $N=3$ remains an open problem.

In anticipation of subsequent publications, it might be mentioned that the $D=1$ results reported here have similarity to behavior in $D=2$ and 3. Numerical studies demonstrate that by inhibiting density fluctuations within a sufficiently large $\mathbf{k}$-space domain around $\mathbf{k}=0$, the particle system is forced to crystallize. But unlike the $D=1$ case, the $D=2$ and 3 cases appear to exhibit a sharp transition (in the large-N limit) between predominately amorphous configurations and clearly crystalline configurations, as the number of vanishing $\rho(\mathbf{k})$'s increases. That is, a phase transition can be induced by changing the range K of repulsive interaction in $\mathbf{k}$ space [Eq. (2.8)].

Finally, we emphasize the desirability of studying the positive-temperature thermal behavior of many-particle systems in $D=1,2$, and 3 with interactions of the form given by Eqs. (2.7) and (2.8).

[1] D. Pines, Solid State Phys. **1**, 367 (1955).
[2] R.P. Feynman, *Statistical Mechanics* (Benjamin, Reading, MA, 1972), pp. 326–330.
[3] M.J. Mandell, J.P. McTague, and A. Rahman, J. Chem. Phys. **64**, 3699 (1976).
[4] J.K. Percus and G.J. Yevick, Phys. Rev. **110**, 1 (1958).
[5] H.C. Andersen and D. Chandler, J. Chem. Phys. **53**, 547 (1970).
[6] *Handbook of Mathematical Functions,* edited by M. Abramowitz and I.A. Stegun (U.S. GPO, Washington, DC, 1964), Chaps. 9 and 10.
[7] L. Brillouin, *Wave Propagation in Periodic Structures* (Dover, New York, 1953).
[8] I. Newton; see, e.g., G. Chrystal, *Textbook of Algebra, Vol. 1* (Chelsea, New York, 1952), Chap. XVIII.
[9] L.D. Landau, Zh. Eksp. Teor. Fiz. **7**, 627 (1937).
[10] S.A. Brazovskii, I.E. Dzyaloshinskii, and A.R. Muratov Zh. Eksp. Teor. Fiz. **93**, 1110 (1987) [Sov. Phys.—JETP **66**, 625 (1987)].
[11] P. Bak, Phys. Rev. Lett. **54**, 1517 (1985).